Traveling Nanoscale Structures in Reactive Adsorbates with Attractive Lateral Interactions

M. Hildebrand, A. S. Mikhailov, and G. Ertl

Fritz-Haber-Institut der Max-Planck-Gesellschaft, Faradayweg 4-6, D-14195 Berlin, Germany

(Received 25 March 1998; revised manuscript received 22 July 1998)

A novel type of traveling structures in surface chemical reactions is presented. These structures, resulting from the competition between reactions, diffusion, and the phase transition caused by attractive lateral interactions between adsorbed particles, are predicted to exist on submicrometer and nanometer scales. We show that internal fluctuations lead to a complex dynamics of interacting wave fragments in this system. [S0031-9007(98)07180-4]

PACS numbers: 82.20.Wt, 05.45.+b, 47.54.+r, 82.65.Jv

The formation of stationary microstructures is often found in systems with potential interactions between particles. At equilibrium, such structures typically result from the competition between short-range attractive and long-range repulsive interactions [1]. Transient microstructured phases spontaneously develop in systems undergoing spinodal decomposition [2,3]. They can be stabilized by introducing nonequilibrium reactions, as has been seen in model simulations of phase-separating reactive binary mixtures [4] and in experiments with polymer blends [5].

A special property of systems far from thermal equilibrium is that, besides stationary structures, they may show oscillations, turbulence, and various wave patterns [6]. Much attention has been paid to studies of traveling waves in various excitable media, including surface chemical reactions [7]. Traveling waves can also softly branch from the homogeneous stationary state through a Hopf bifurcation with a broken translational symmetry (we call it the "wave bifurcation"). Wave bifurcations have already been found in various problems, such as binary-fluid convection [8] or electrically driven nematic liquid crystals [9]. The detailed mathematical analysis of pattern selection and modulational instabilities in the postbifurcation regimes has been performed [10–12], and the role of noises in these regimes has been discussed [13].

Interactions between adsorbed atoms and molecules on metal surfaces are often mediated through the substrate, and their range can extend from several angstroms to several nanometers [14]. As has been observed in recent scanning tunneling microscopy experiments [15], such attractive interactions may be strong enough to induce nanoscale phase separation. Earlier we developed a mesoscopic theoretical approach for the description of reactive adsorbates with potential interactions between particles involving nonlinear nonlocal Langevin evolution equations for fluctuating adsorbate coverages [16,17] (see also [18]). This mesoscopic approach has been applied by us to study the motion of interfaces and spontaneous nucleation in nonreactive adsorbates undergoing a first-order phase transition [17]. It has also been used to investigate the formation of stationary microstructures of different morphologies in adsorbates with chemical reactions [19].

In the present paper we show that a wave bifurcation can lead to the formation of traveling submicrometer and nanoscale structures in surface chemical reactions with sufficiently strong attractive lateral interactions between adsorbed particles. We consider a hypothetical model system with two adsorbed species (U and V) that participate in the nonequilibrium annihilation reaction $U + V \rightarrow 0$. The reaction product immediately escapes the surface, leaving two free surface sites. The particles U and V occupy different sets of adsorption sites. Both species are continuously supplied by adsorption from the gas phase. The particles V are so strongly chemisorbed that they do not desorb thermally and cannot laterally move across the surface. On the other hand, the particles U are only weakly bound to the substrate; they are highly mobile and can desorb. An essential property of the model is that it includes potential interactions between the particles. We assume that particles U are strongly attracting each other and, in the absence of the other species V, this adsorbate would undergo a first-order phase transition. The particles of the second species V are attracted to particles U but do not interact among themselves. Assuming linear transition rates, the following mesoscopic evolution equations for the fluctuating coverages u and v are obtained (cf. [17]) for this system:

$$\frac{\partial u}{\partial t} = k_{\mathrm{ad}}^{u} p_u (1 - u) - k_{\mathrm{des}}^{u}(W) u - k_r u v + D\nabla^2 u + \nabla\left[\frac{D}{k_B T}\, u(1 - u)\nabla W(\mathbf{r})\right] + \xi_u(\mathbf{r}, t), \quad (1)$$

$$\frac{\partial v}{\partial t} = k_{\mathrm{ad}}^{v} p_v (1 - v) - k_r u v + \xi_v(\mathbf{r}, t).$$

Here k_{ad}^{u} and k_{ad}^{v} are the sticking coefficients of the species U and V, p_u and p_v are their constant partial pressures in the gas phase, k_r is the reaction rate constant, D is the diffusion constant of the mobile species U, and T is the temperature. The desorption rate coefficient $k_{\mathrm{des}}^{u}(W)$ for the particles of type U depends on the local potential $W(\mathbf{r})$ as $k_{\mathrm{des}}^{u}(W) = k_{\mathrm{des}}^{u} \exp[W(\mathbf{r})/k_B T]$. This potential acting on adsorbed particles U results from attractive pairwise interactions with surrounding

 0031-9007/98/81(12)/2602(4)$15.00

molecules of the species U and V and is given by $W(\mathbf{r}) = -\int w_{uu}(\mathbf{r}-\mathbf{r}')u(\mathbf{r}')\,d\mathbf{r}' - \int w_{uv}(\mathbf{r}-\mathbf{r}')v(\mathbf{r}')\,d\mathbf{r}'$. For simplicity we assume that both binary interactions have the same radius r_0, although their strengths are different. The interactions are therefore described by functions $w_{uu}(r) = (w_{uu}^0/\pi r_0^2)\exp(-r^2/r_0^2)$, and $w_{vv}(r) = (w_{vv}^0/\pi r_0^2)\exp(-r^2/r_0^2)$. We note that, besides the diffusion term, the evolution equation for the mobile species U also contains a term describing a drift of this adsorbed species in the gradient of the local potential.

The internal noises $\xi_u(\mathbf{r},t)$ and $\xi_v(\mathbf{r},t)$ in the mesoscopic equations (1) take into account fluctuations of adsorption, desorption, reaction, and diffusion processes which are defined as discrete stochastic processes on the underlying lattice and are described by the respective microscopic master equation for joint probability distributions (see [17]),

$$\begin{aligned}\xi_u(\mathbf{r},t) &= Z^{-1/2}\sqrt{k_{\mathrm{ad}}^u(1-u)}\,f_{\mathrm{ad}}(\mathbf{r},t) + Z^{-1/2}\sqrt{k_{\mathrm{des}}^u u\,\exp[W(\mathbf{r})/k_BT]}\,f_{\mathrm{des}}(\mathbf{r},t)\\ &\quad + Z^{-1/2}\sqrt{k_r uv}\,q_{\mathrm{react}}(\mathbf{r},t) + Z^{-1/2}\nabla[\sqrt{Du(1-u)}\,\mathbf{f}(\mathbf{r},t)],\\ \xi_v(\mathbf{r},t) &= Z^{-1/2}\sqrt{k_{\mathrm{ad}}^v(1-u)}\,g_{\mathrm{ad}}(\mathbf{r},t) + Z^{-1/2}\sqrt{k_r uv}\,q_{\mathrm{react}}(\mathbf{r},t).\end{aligned} \tag{2}$$

All these noises are proportional to $Z^{-1/2}$, where Z is the lattice density, i.e., the number of lattice sites per unit surface area of the metal substrate. Hence, $l_0 = 1/\sqrt{Z}$ is the atomic lattice length representing an important microscopic parameter of the problem. Note that the mesoscopic evolution equations are derived through coarse graining of the microscopic master equation over area elements containing a large number of lattice sites but still small if compared with the interaction radius r_0. It is therefore applicable only if the condition $r_0 \gg l_0$ is satisfied [17]. The random forces $\mathbf{f}$, f_{ad}, f_{des}, g_{ad}, and q_{react} in Eqs. (2) represent independent white noises of unit intensity; i.e., we have $\langle f_{\mathrm{ad}}(\mathbf{r},t)f_{\mathrm{ad}}(\mathbf{r}',t')\rangle = \langle f_{\mathrm{des}}(\mathbf{r},t)f_{\mathrm{des}}(\mathbf{r}',t')\rangle = \langle q_{\mathrm{react}}(\mathbf{r},t)q_{\mathrm{react}}(\mathbf{r}',t')\rangle = \langle f_x(\mathbf{r},t)f_x(\mathbf{r}',t')\rangle = \langle f_y(\mathbf{r},t)\times f_y(\mathbf{r}',t')\rangle = \langle g_{\mathrm{ad}}(\mathbf{r},t)g_{\mathrm{ad}}(\mathbf{r}',t')\rangle = \delta(\mathbf{r}-\mathbf{r}')\delta(t-t')$, and $\langle f_x(\mathbf{r},t)f_y(\mathbf{r}',t')\rangle = 0$. The reaction-related noises in the equations for the coverages u and v are identical because each annihilation event simultaneously changes the numbers of particles of both species.

To simplify the analysis, we measure time in units of the mean surface residence time $(k_{\mathrm{des}}^u)^{-1}$ of particles U. The surface coordinates are measured in units of the characteristic diffusion length $L_{d,u} \equiv \sqrt{D/k_{\mathrm{des}}^u}$ of particles U with respect to their desorption. The studied system is then characterized by several dimensionless parameters $\alpha = k_{\mathrm{ad}}^u p_u/k_{\mathrm{des}}^u$, $\kappa = k_r/k_{\mathrm{ad}}^u p_u$, $\beta = k_{\mathrm{ad}}^v p_v/k_r$, $\varepsilon = w_{uu}^0/k_BT$, $\varepsilon' = w_{uv}^0/k_BT$, and $\rho_0 = r_0/L_{d,u}$.

We consider first the phenomena described by Eqs. (1) in the deterministic limit, neglecting fluctuations. The stationary uniform states $u = u_0$ and $v = v_0$ of this system are obtained in terms of the dimensionless parameters by solving the equation $\alpha[1-u-\kappa u v_0(u)] - u\exp[-\varepsilon u - \varepsilon' v_0(u)] = 0$, where $v = v_0(u) = \beta/(\beta+u)$. Inside the cusp region shown by the solid curve in Fig. 1, the system has a dense and a dilute uniform phase. Outside that region, it has only one uniform phase.

The stability of these uniform states is tested by adding small plane-wave perturbations with wave number k and linearizing Eqs. (1). At the instability boundary, the growth rate of these perturbations, i.e., the largest real part of the eigenvalues λ_k of the corresponding Jacobian, becomes positive for a mode with a certain wave number k_0. Figure 2 shows the largest real part and the respective imaginary part of λ_k near the instability point. We see that, in contrast to the standard Turing bifurcation, the first unstable mode has a finite oscillation frequency. This is the characteristic property of the wave bifurcation (see [11]).

In the limit $\rho_0 \to 0$ the instability boundary of the uniform phases is determined by the condition $u_0 = u_D$, where $u_D \equiv (1-\sqrt{1-4/\varepsilon})/2$. As the reaction rate constant is increased, the instability first develops in a small region close to the critical cusp point in the parameter plane (ε,α). Subsequently, the instability region grows and spreads over a large part of this parameter plane. As an example, Fig. 1 shows the instability boundaries in the limit $\rho_0 \to 0$ in this case. When the dimensionless interaction radius ρ_0 is sufficiently small, the wave number k_0 of the first unstable mode is approximately given in the

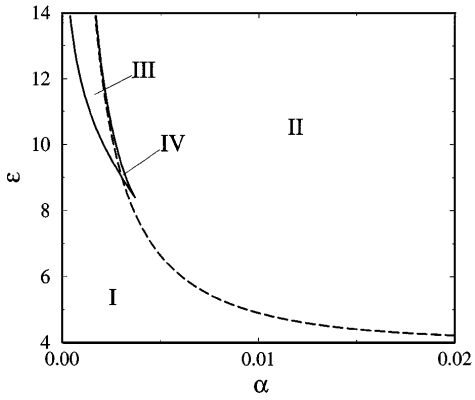

FIG. 1. Bifurcation diagram in the parameter plane (ε,α) for $\varepsilon' = 3$, $\beta = 3$, and $\kappa = 1$. Two uniform states of the system are found inside the cusp shown by the solid curve. The dashed line corresponds to the wave bifurcation in the limit $\rho_0 \to 0$. In region I the system has a single uniform phase, in II a single type of traveling wave train is found, in III one uniform low-density state coexists with wave trains, and in IV two different types of traveling wave trains coexist.

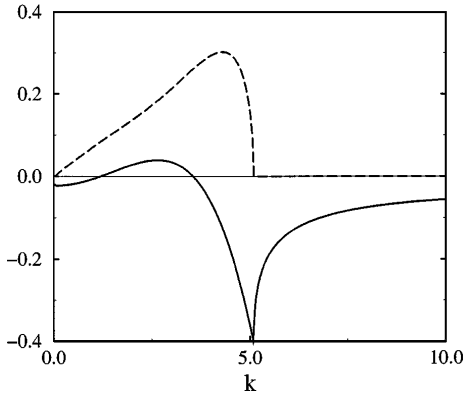

FIG. 2. Dispersion relation for $\varepsilon = 5$, $\varepsilon' = 3$, $\beta = 3$, $\kappa = 1$, $\alpha = 0.01$, and $r_0 = 0.01 L_{\mathrm{diff}}$. The bold solid line shows $\mathrm{Re}(\lambda_k)$, and the dashed line displays the imaginary part $\mathrm{Im}(\lambda_k)$ as functions of the wave number k.

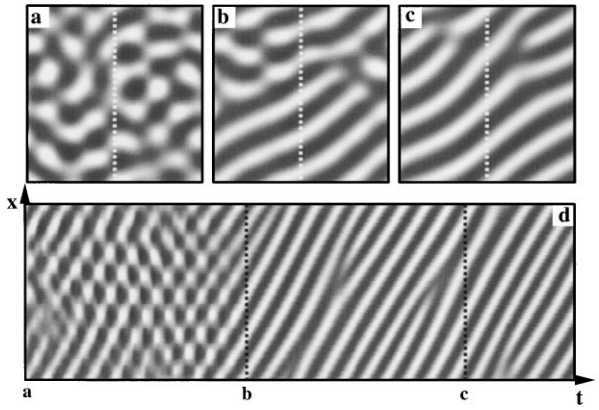

FIG. 3. Formation of coherent traveling wave patterns at $\varepsilon = 5$, $\varepsilon' = 3$, $\kappa = 1$, $\beta = 3$, $\alpha = 0.5$, and $r_0 = 0.07 L_{\mathrm{diff}}$. Snapshots (a), (b), and (c) correspond to time moments: (a) $t = 18/k^u_{\mathrm{des}}$; (b) $t = 45/k^u_{\mathrm{des}}$; (c) $t = 72/k^u_{\mathrm{des}}$. The temporal evolution in (d) is displayed during the time interval $18/k^u_{\mathrm{des}} < t < 85/k^u_{\mathrm{des}}$ in the one-dimensional cross section indicated by the vertical dashed lines in the snapshots. The total size of the system is $L = 4.2 L_{\mathrm{diff}}$. The local surface coverage of the species U is shown in gray scale, with darker areas corresponding to higher coverages.

nonrescaled units by

$$k_0 = 2^{1/2}(\varepsilon u_D \upsilon_D + \beta + u_D)^{1/4}(r_0 L_{\mathrm{diff}})^{-1/2}, \qquad (3)$$

where the characteristic diffusion length of the reaction $L_{\mathrm{diff}} = \sqrt{D/k_r}$ and the notation $\upsilon_D = \beta/(\beta + u_D)$ are introduced.

The analysis of the bifurcation diagrams shows that a minimum reaction rate and a small enough interaction radius are necessary in order to observe the considered instability. Furthermore, when the characteristic intensity ε' of the cross-species interactions is decreased, a codimension-2 bifurcation is found at $\varepsilon'_{\mathrm{crit}}$. For sufficiently small ρ_0 this critical value is approximately given by $\varepsilon'_{\mathrm{crit}} = 2\varepsilon(\beta^2 \upsilon_D^{-3} + u_D) L_{\mathrm{diff}}^{-2}(k_0^2 + k_t^2)^{-1}$, where $k_t = 2^{1/2}[\upsilon_D/(1 - u_D) - u_D \upsilon_D^2/\beta]^{1/4}(r_0 L_{\mathrm{diff}})^{-1/2}$ is the critical wave number at the Turing bifurcation. At weaker cross interactions between the two species, the instability leading to stationary microstructures is first taking place. Indeed, in the limit when $\beta \to \infty$ and $\varepsilon' = 0$, the considered system reduces to the previously studied model where only stationary microstructures were possible [19].

We have performed numerical simulations of the deterministic system in the unstable region for $\varepsilon' > \varepsilon'_{\mathrm{crit}}$ using periodic boundary conditions. Our one-dimensional simulations reveal, in this case, the development of periodic wave trains traveling at a constant velocity. Figure 3 displays the results of a typical two-dimensional simulation in the absence of fluctuations, starting with small random perturbations added to the unstable homogeneous phase. Three snapshots [Figs. 3(a), 3(b), and 3(c)] show the coverage distribution of the species U at different selected time moments in the entire system. To characterize the dynamic behavior of the patterns, Fig. 3(d) presents the temporal evolution along the cross section shown by the dashed lines in these three snapshots.

It can be seen that, at the early stage of evolution from the unstable uniform state, irregular patterns of distorted standing waves are formed [Fig. 3(a)]. Later, however, the standing waves evolve into planar wave trains traveling at a constant velocity. These wave trains tend to form a periodic pattern containing pointlike defects. Note that the characteristic scales of this wave pattern can be very small. In this simulation the interaction radius is $r_0 = 0.07 L_{\mathrm{diff}}$, and the resulting characteristic wavelength of the wave train is about $0.75 L_{\mathrm{diff}}$, i.e., shorter than the diffusion length of the system. It can be made even much shorter by further decreasing the interaction radius [cf. Eq. (3)].

Generally, selection and stability of patterns above the wave bifurcation can be studied by means of coupled dynamical equations for the amplitudes of interacting unstable modes representing left- and right-propagating waves [10–12]. Depending on the coefficients of these equations, the system forms either standing or traveling waves. Moreover, the patterns may also be unstable with respect to a modulational instability. We have derived in the one-dimensional case the amplitude equations for the considered system when thermal desorption of the species U is absent and have analytically determined the coefficients of these equations. This analysis shows that there are large regions in the parameter space where the bifurcation is supercritical. In these regions the interaction between the modes leads to the selection of traveling waves which are stable with respect to spatial modulations of their amplitudes. Thus, the results of this preliminary study support our numerical findings.

The traveling patterns can be much smaller than the characteristic diffusion length which itself may be on the submicrometer scale. In such a situation only a relatively small number of adsorbed particles contributes

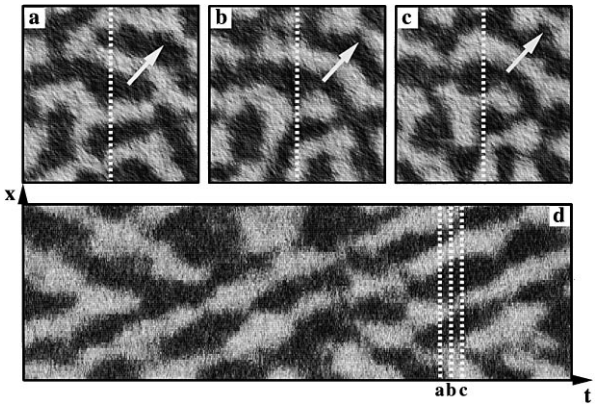

FIG. 4. Fluctuating traveling wave fragments: $Z = (1.07 \times 10^5) L_{\mathrm{diff}}^{-2}$, $\alpha = 0.08$, $L = 1.7 L_{\mathrm{diff}}$, and $r_0 = 0.028 L_{\mathrm{diff}}$; the other parameters are the same as in Fig. 3. The two-dimensional snapshots (a), (b), and (c) are separated by equal intervals $\Delta t = 0.89/k_{\mathrm{des}}^u$. The temporal evolution in the one-dimensional cross section (d) is shown during time $t = 44.6/k_{\mathrm{des}}^u$.

to the formation of a specific pattern, and, hence, internal fluctuations have to be taken into account. Figure 4 shows the fluctuating coverage distributions in the asymptotic statistical regime obtained by numerical integration of Eqs. (1) including the noise terms given by Eqs. (2). Here the interaction radius r_0 is equal to only nine atomic lattice lengths l_0; the total size of the system is $L = 555 l_0$, and the characteristic diffusion length is $L_{\mathrm{diff}} = 327 l_0$. Clearly, at these small scales the internal noises of the diffusion, adsorption, desorption, and reaction processes exhibit strong influence on the patterns. The individual traveling stripes are now broken into many short fragments that form irregular spatial patterns seen in the snapshots [Figs. 4(a), 4(b), and 4(c)]. Nonetheless, examining the time evolution in the central cross section [Fig. 4(d)], we recognize that these fragments do not just fluctuate. These microstructures *travel across the surface* while undergoing irregular variations of their shapes. The directions of the translational motion of different fragments are random, and the fragments often collide. Merging of traveling fragments, as well as splitting events, is observed in this process. Remarkably, the magnitude of the propagation velocity of different fragments does not significantly differ.

Thus, we have shown within the framework of a hypothetical model that the presence of strong attractive lateral interactions in reacting adsorbates can lead to the spontaneous formation of traveling wave fragments on submicrometer and nanometer scales. The experimental observation of such traveling microstructures can be an interesting problem for the next generation of high-resolution photoelectron emission microscopes.

The analogies between adsorbates and phase-separating polymer blends or Langmuir-Blodgett layers [20] suggest that similar mechanisms may produce traveling nanoscale structures in other soft matter far from equilibrium. Such extremely small traveling structures would fit perfectly into the characteristic dimensions of a single biological cell and may therefore play an important functional role by providing additional possibilities for information transfer and intracellular transport of particles (see also [21,22]).

The authors thank D. Walgraef for a discussion of mathematical aspects of the wave bifurcation. We are grateful to M. Scheffler for providing access to CRAY-T3E in Garching.

[1] M. Seul and D. Andelman, Science **267**, 476 (1995), and references therein.
[2] J. W. Cahn, Acta Metall. **9**, 795 (1961).
[3] K. Binder, in *Material Science and Technology: Phase Transformations in Materials*, edited by P. Haasen (VCH, Weinheim, 1990), Vol. 5, p. 405.
[4] S. C. Glotzer, E. A. Di Marzio, and M. Muthukumar, Phys. Rev. Lett. **74**, 2034 (1995); M. Motoyama and T. Ohta, J. Phys. Soc. Jpn. **66**, 2715 (1997).
[5] Q. Tran-Cong and A. Harada, Phys. Rev. Lett. **76**, 1162 (1996).
[6] *Chemical Waves and Patterns*, edited by R. Kapral and K. Showalter (Kluwer Academic Publishers, Dordrecht, The Netherlands, 1995).
[7] R. Imbihl and G. Ertl, Chem. Rev. **95**, 697 (1995).
[8] M. C. Cross, Phys. Rev. Lett. **57**, 2935 (1986).
[9] E. Bodenschatz, W. Zimmermann, and L. Kramer, J. Phys. (France) **49**, 1875–1899 (1988).
[10] A. C. Newell, in *Lecture Notes in Applied Mathematics* (Springer-Verlag, Berlin, 1974), Vol. 15, p. 157.
[11] D. Walgraef, *Spatio-Temporal Pattern Formation* (Springer-Verlag, Berlin, 1997).
[12] E. Knobloch and J. de Luca, Nonlinearity **3**, 975 (1990).
[13] M. Neufeld, D. Walgraef, and M. San Miguel, Phys. Rev. E **54**, 6344 (1996).
[14] See, e.g., J. K. Nørskov, in *Coadsorption, Promoters and Poisons*, edited by D. A. King and D. P. Woodruff (Elsevier, Amsterdam, 1993), p. 1.
[15] J. Trost, T. Zambelli, J. Wintterlin, and G. Ertl, Phys. Rev. B **54**, 17 850 (1996); J. Wintterlin, J. Trost, S. Renisch, R. Schuster, T. Zambelli, and G. Ertl, Surf. Sci. **394**, 159 (1997).
[16] A. S. Mikhailov and G. Ertl, Chem. Phys. Lett. **238**, 104 (1995).
[17] M. Hildebrand and A. S. Mikhailov, J. Phys. Chem. **100**, 19 089 (1996).
[18] G. Giacomin and J. L. Lebowitz, Phys. Rev. Lett. **76**, 1094 (1996).
[19] M. Hildebrand, A. S. Mikhailov, and G. Ertl, Phys. Rev. E (to be published).
[20] A. S. Mikhailov and G. Ertl, Science **272**, 1596 (1996).
[21] B. Hess and A. S. Mikhailov, Science **264**, 223 (1994).
[22] B. Alberts, Cell **92**, 291 (1998).